Influence of decorrelation on Heisenberg-limited interferometry with quantum correlated photons

Taesoo Kim,* Olivier Pfister,† Murray J. Holland, Jaewoo Noh,‡ and John L. Hall
JILA, University of Colorado and National Institute of Standards and Technology, Boulder, Colorado 80309-0440
(Received 5 May 1997; revised manuscript received 29 December 1997)

The feasibility of a Heisenberg-limited phase measurement using a Mach-Zehnder interferometer fed with twin photon correlated light is investigated theoretically. To take advantage of the Heisenberg limit, $1/N$, for the phase sensitivity, one wants the number of correlated photons, N, to be high. This favors the use of parametric oscillation rather than the weaker but better correlated source given by parametric down-conversion. In real systems, decorrelation arising from photon absorption, mode mismatch, and nonideal detectors must be considered. In this paper we address the problem of detection when correlated photons are used as the input. We study the influence of photon statistics and of imperfect quantum correlation of the input light, and show that it is still possible to break the classical $1/\sqrt{N}$ phase sensitivity limit in nonideal experimental conditions. All the results are valid in the general case of quantum correlated bosons. [S1050-2947(98)09805-9]

PACS number(s): 42.50.Dv, 03.75.−b, 03.75.Fi

I. INTRODUCTION

The precise measurement of phase at the quantum level is an issue of fundamental importance for both theory and experiment. As well as being a research subject by itself in quantum optics, the measurement of phase through interference is a ubiquitous topic in physics. Extremely accurate methods of measuring optical phase through interferometry are required for gravitational wave detection experiments. The precision to which the phase of a matter field can be measured is important in atomic interferometry and Ramsey fringe experiments as well as internal interference experiments in ion traps. Spontaneous symmetry breaking in condensed matter systems produces a well-defined condensate phase and dominates low-temperature phenomena in superfluids, giving rise to interference effects such as in the Josephson junction. Finally, issues of phase detectability and quantum fluctuations are currently of high interest in Bose-Einstein condensation experiments in dilute atomic vapors, where the fundamental quantum limits on phase resolution arising from finite number are important.

All phase dependent observables are generated by interference experiments that involve summing amplitudes of fields that may take alternate paths. A generic model that can be studied in detail is the Mach-Zehnder interferometer [1], which is a four-port optical device. A limit to phase resolution arises from the minimum detectable phase difference between the path lengths in the arms of the interferometer when it is fed, for example, by a coherent state such as that generated in a laser. This is not optimal for phase resolution experiments because only one input port is used: vacuum fluctuations enter the unused port and are amplified in the interferometer by the coherent field. The phase measurement sensitivity of this system cannot exceed what is usually called the standard limit (SL),

$$\Delta\theta_{\mathrm{SL}} \sim \frac{1}{\sqrt{N}}, \tag{1}$$

which is independent of the photon statistics of the input light [2] . Several schemes to reduce the phase uncertainty below this limit have been proposed. One solution is to squeeze the vacuum entering the unused port [3,4]. Xiao *et al.* [5] and Grangier *et al.* [6] have used an optical parametric oscillator (OPO) below threshold for this purpose and demonstrated experimental increases of sensitivity of, respectively, 3 and 2 dB beyond the SL. The unsurpassable limit is eventually the Heisenberg limit (HL),

$$\Delta\theta_{\mathrm{HL}} \sim \frac{1}{N}, \tag{2}$$

which, as we will see, can be qualitatively viewed as stemming from the number-phase Heisenberg uncertainty between the phase difference and the intensity difference between the two arms of the interferometer. Solutions other than squeezing the vacuum input have been proposed to approach the HL [7–11]. In Ref. [9], Holland and Burnett suggested using an input state containing correlated identical (twin) photons entering each input port. Such states can be produced by type-II, frequency degenerate, parametric down-conversion (PDC) or oscillation (OPO). The latter presents the advantage of the OPO-cavity buildup producing large numbers of photons, which increase the sensitivity according to Eq. (2). However, intracavity losses are also amplified and partially decorrelate the output field. In this paper, we analyze the effects on phase sensitivity of partial correlation and random deletion of photon pairs, as well as the effect of the photon statistics of the input state.

*Permanent address: Department of Physics, University of Ulsan, Ulsan 680-749, Korea.
†Present address: Department of Physics, Duke University, Box 90305, Durham, NC 27708.
‡Permanent address: Department of Physics, Inha University, Inchon 402-751, Korea.

It is worth noting that, although we take the Mach-Zehnder interferometer as our system, these results are general. Indeed, the above limits apply whenever one observes a phase shift of a quantum coherence. Examples of such situations are interference experiments using trapped ions [12], or atomic interferometry with Bose condensates [13]. In these two cases, the field is a matter wave. Any example may be thought of as a unitary transformation of a pair of quantum states. This leads to a common mathematical formalism, using SU(2) matrices that can be made equivalent to tridimensional rotations by use of the Schwinger representation.

In Secs. II and III A, we review this formalism and apply it to the Mach-Zehnder interferometer, essentially recalling the work of Yurke *et al.* [7], except in Sec. II A 2, where we outline the physical meaning of the Schwinger representation and interpret it in terms of a number-phase Heisenberg uncertainty. We then apply the formalism to the correlated input photons scheme proposed in [9]. In Sec. III B, we use the physical interpretation of Sec. II A 2 to give a hand-waving analysis of the influence of single- and twin-input states on the sensitivity of the interferometer. We insist on the point that the term ''phase'' throughout this paper always refers to a classical number. The definition of quantum phase is still an open question [14], but no such definition is in fact needed in the context of this work. We then consider, in Sec. III C, experimental interferometric measurements with a quantum-correlated input. We derive the phase uncertainty and the signal-to-noise ratio of a direct detection: if the former is indeed the HL, the latter should, however, be very low. This issue can be solved by the use of Bayesian data processing [9]. In Sec. IV, we investigate this procedure to determine the feasability of a Heisenberg-limited measurement in the case of nonideal experimental conditions (imperfect photon correlation and detection efficiency) and for different input photon statistics.

II. PRESENTATION OF THE FORMALISM

We use the very elegant description of four-port optical systems, in terms of rotations in an abstract tridimensional space, that was demonstrated by Yurke *et al.* [7]. This formalism also carries a straightforward physical meaning that is analogous to that of the Bloch vector for a two-level atomic system, or of the polarization vector spanning the Poincaré sphere.

The key point is that any passive lossless four-port optical system can be described by a 2×2 special unitary matrix.[1] This matrix operates on a bidimensional vector, whose components are the two field amplitudes at each port of the system:

$$\begin{pmatrix} a_{\rm out} \\ b_{\rm out} \end{pmatrix} = \begin{pmatrix} \cos\frac{\beta}{2} e^{i(\alpha+\gamma)/2} & \sin\frac{\beta}{2} e^{i(\alpha-\gamma)/2} \\ -\sin\frac{\beta}{2} e^{-i(\alpha-\gamma)/2} & \cos\frac{\beta}{2} e^{-i(\alpha+\gamma)/2} \end{pmatrix} \times \begin{pmatrix} a_{\rm in} \\ b_{\rm in} \end{pmatrix}. \tag{3}$$

α, β, and γ are the Euler angles [15], whose physical meaning will be explained for practical optical systems later on. The components (a_i, b_i) are annihilation operators satisfying boson comutation relations. We take all fields to have the same frequency and polarization.

A. The Schwinger representation

1. Definition

The Schwinger representation makes use of the correspondence between the SU(2) and SO(3) groups: the general rotation given in Eq. (3) can be viewed as the rotation of the following tridimensional vector,

$$\boldsymbol{J} = \begin{pmatrix} J_x \\ J_y \\ J_z \end{pmatrix} = \frac{1}{2} \begin{pmatrix} a^\dagger b + b^\dagger a \\ -i(a^\dagger b - b^\dagger a) \\ a^\dagger a - b^\dagger b \end{pmatrix}. \tag{4}$$

$\boldsymbol{J}$ is a quantum angular momentum, which is proven by the canonical comutation relations

$$[J_x, J_y] = iJ_z, \ \text{ etc.} \tag{5}$$

The square modulus of $\boldsymbol{J}$ is

$$J^2 = \frac{a^\dagger a + b^\dagger b}{2} \left(\frac{a^\dagger a + b^\dagger b}{2} + 1 \right) \tag{6}$$

$$= \frac{N_a + N_b}{2} \left(\frac{N_a + N_b}{2} + 1 \right), \tag{7}$$

where $N_a = a^\dagger a$ $(N_b = b^\dagger b)$ is the photon number operator for port a (b).

2. Physical meaning of J

J^2 is related to the total number of photons in the system. Its conservation means conservation of the total number of photons in the whole optical system. J_z is the intensity difference between ports a and b. $J_{x,y}$ (and $J_\pm = J_x \pm iJ_y$) are quadrature interference terms of the fields E_a and E_b and are therefore pointing to the phase difference between the two fields. This is easily seen from the following: one writes

$$E_a = E_a^{(+)} - E_a^{(-)} = a e^{i\phi_a} - a^\dagger e^{-i\phi_a}, \tag{8}$$

$$E_b = E_b^{(+)} - E_b^{(-)} = b e^{i\phi_b} - b^\dagger e^{-i\phi_b}, \tag{9}$$

where ϕ_a and ϕ_b are real numbers, and a and b quantum

[1] Unitarity stems from the conservation of energy between the input and output ports.

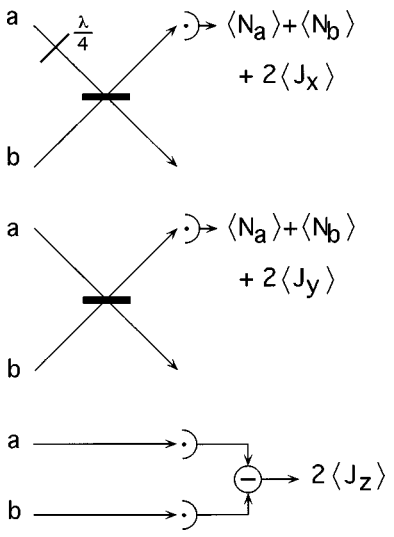

FIG. 1. Physical meaning of the Schwinger representation: what the three components $J_{x,y,z}$ mean in terms of optical measurements.

annihilation operators. The photodetection term at the output of a beam splitter (Fig. 1, top) is

$$[E_a^{(-)}+E_b^{(-)}][E_a^{(+)}+E_b^{(+)}]$$
$$=N_a+N_b+J_+e^{i(\phi_a-\phi_b)}+J_-e^{-i(\phi_a-\phi_b)} \tag{10}$$

$$=N_a+N_b+2J_x\cos(\phi_a-\phi_b)+2J_y\sin(\phi_a-\phi_b), \tag{11}$$

which demonstrates that $J_{x,y}$ describe the interference between E_a and E_b. Figure 1 displays the measurement schemes associated to each component of $\boldsymbol{J}$, assuming coherent states for the two fields and $\phi_a=\phi_b$ at the input. If one considers Fock states rather than coherent states, then the phase of each input field is undetermined and no information about the phase difference can be obtained either (the interference terms $\langle J_x\rangle=\langle J_y\rangle=0$ in Fig. 1). However, this only applies to the *input* fields of Fig. 1. We will see that, in the two measurement schemes on the top of Fig. 1, the *output* beams (which, exiting a beam splitter, can in fact be considered as being inside a Mach-Zehnder interferometer) have a phase difference that can be very well determined and measured, even for Fock states. This is due, as we will see in Sec. II B 1, to the property of a beam splitter to swap intensity and phase fluctuations between the input and output beams.

It is also interesting to note that the standard Heisenberg uncertainty relation

$$\Delta J_z\Delta J_x\geqslant\frac{1}{2}|\langle J_y\rangle| \tag{12}$$

has the physical meaning of the Heisenberg uncertainty relation between the photon number difference and the phase difference of the two fields,

$$\Delta(N_a-N_b)\Delta(\phi_a-\phi_b)\geqslant 1. \tag{13}$$

Equation (13) is derived from the time-energy Heisenberg uncertainty [16], $\phi_a-\phi_b$ being a *classical* variable.[2] We point out, however, that Eq. (13) is also connected, by the above qualitative argument, to the *operatorial* angular momentum uncertainty (12).

3. Eigenstates of J

According to what precedes, the choice of z as the quantization axis for $\boldsymbol{J}$ means that one chooses to measure the intensity difference with the highest precision, therefore allowing a maximum uncertainty on the phase difference. On the contrary, choosing x or y means optimally defining the phase difference at the expense of the knowledge of the intensity difference. We choose here to quantize along z, since J_z is the observable measured in the experiment, as we will see later.

Unsurprisingly, the eigenstates of J^2 and J_z are identical to the eigenstates of N_a and N_b,

$$|n_an_b\rangle=|j\mu\rangle_z, \tag{14}$$

where n_a and n_b are the eigenvalues of N_a and N_b, respectively. The eigenvalue of J^2 is $j(j+1)$, and the eigenvalue of J_z is μ where

$$j=\frac{n_a+n_b}{2}=\frac{N}{2}, \tag{15}$$

$$\mu=\frac{n_a-n_b}{2}. \tag{16}$$

We always note N the total number of photons flowing in the interferometer, and take N even. Two simple examples that we use throughout this paper are the Fock single-input state,

$$|N0\rangle=|jj\rangle_z, \tag{17}$$

and the Fock twin-photon input,

$$\left|\frac{N}{2}\,\frac{N}{2}\right\rangle=|j0\rangle_z, \tag{18}$$

B. Optical four-port elements as rotation operators

In the Schwinger representation, the general rotation of Eq. (3) is equivalent, in the Heinsenberg picture, to

$$\boldsymbol{J}^{\text{out}}=e^{i\alpha J_z}e^{i\beta J_y}e^{i\gamma J_z}\boldsymbol{J}^{\text{in}}e^{-i\gamma J_z}e^{-i\beta J_y}e^{-i\alpha J_z}, \tag{19}$$

and, in the Schrödinger picture, to

$$|\psi_{\text{out}}\rangle=e^{-i\alpha J_z}e^{-i\beta J_y}e^{-i\gamma J_z}|\psi_{\text{in}}\rangle. \tag{20}$$

Both pictures are equivalent in the sense that rotating operators by $+\theta$ is equivalent to rotating states by $-\theta$. Two examples of interest for the further description of an interferometer are the beam splitter and the phase shift.

[2]The derivation of an operatorial version of Eq. (13) poses problems that are outside the scope of this paper [14].

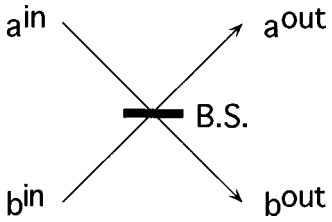

FIG. 2. Input and output ports of the beam splitter.

1. Beam splitter

The symmetric lossless beam splitter (Fig. 2) introduces a $\pi/2$ phase shift between the reflected and the transmitted beams. It is described by the SU(2) matrix

$$\begin{pmatrix} a_{\rm out} \\ b_{\rm out} \end{pmatrix} = \begin{pmatrix} r & \pm it \\ \pm it & r \end{pmatrix} \begin{pmatrix} a_{\rm in} \\ b_{\rm in} \end{pmatrix}, \tag{21}$$

where r and t are the square roots of the Fresnel intensity coefficients for reflection and transmission ($r^2+t^2=1$). This corresponds to Eq. (3) with $\alpha=-\gamma=\pi/2$, $\beta=\pm\varphi=\pm 2\arccos r$ ($0\leqslant\varphi\leqslant\pi$), which gives the SU(2) matrix

$$\begin{pmatrix} a_{\rm out} \\ b_{\rm out} \end{pmatrix} = \begin{pmatrix} \cos\dfrac{\varphi}{2} & \pm i\sin\dfrac{\varphi}{2} \\ \pm i\sin\dfrac{\varphi}{2} & \cos\dfrac{\varphi}{2} \end{pmatrix} \begin{pmatrix} a_{\rm in} \\ b_{\rm in} \end{pmatrix}. \tag{22}$$

The corresponding SO(3) rotation is

$$\begin{pmatrix} J_x^{\rm out} \\ J_y^{\rm out} \\ J_z^{\rm out} \end{pmatrix} = \begin{pmatrix} 1 & 0 & 0 \\ 0 & \cos\varphi & \pm\sin\varphi \\ 0 & \mp\sin\varphi & \cos\varphi \end{pmatrix} \begin{pmatrix} J_x^{\rm in} \\ J_y^{\rm in} \\ J_z^{\rm in} \end{pmatrix}, \tag{23}$$

which is equivalent to rotating the light state by $\pm\varphi$ around x. Of most interest is the case of a 50/50 ($r=t=1/\sqrt{2}$) beam splitter, which gives a $\pm\pi/2$ rotation around the x axis. This can be written from Eq. (19),

$$J_z^{\rm out} = e^{\mp i(\pi/2)J_x} J_z^{\rm in} e^{\pm i(\pi/2)J_x} = \mp J_y^{\rm in}, \tag{24}$$

or, according to Eq. (20), with $|\psi_{\rm in}\rangle_z = |j\,\mu\rangle_z$,

$$|\psi_{\rm out}\rangle = e^{\pm i(\pi/2)J_x}|j\,\mu\rangle_z = |j\ \ \pm\mu\rangle_y. \tag{25}$$

From Sec. II A 2, Eq. (24) proves that measuring the intensity difference at the output of a beam splitter gives information about the phase difference at its input, and conversely (other demonstrations are given by Holland and Burnett [9] and Hillery *et al.* [17], for classical and quantum fields). Therefore, since the region where one probes the phase shift θ of a Mach-Zehnder interferometer lies between two beam splitters, one only needs to worry about the quantum properties of the *intensity* of the light, before and after these beam splitters, to obtain information about θ. There is thus no need for a definition of a quantum phase operator to model the interferometric measurements discussed in this paper.

To illustrate further the beam splitter in the Schwinger representation, we give two simple examples, using the rotation matrix elements $d^j_{\mu'\mu}(\varphi) = \langle j\,\mu'|e^{-i\varphi J_y}|j\,\mu\rangle$ [15]. The single photon input state $|10\rangle = |\frac{1}{2}\,\frac{1}{2}\rangle_z$ gives the following output state under the beam-splitter transformation:

$$\begin{aligned} e^{i(\pi/2)J_x}\left|\frac{1}{2}\,\frac{1}{2}\right\rangle_z &= e^{-i(\pi/4)} \sum_{\mu=-\frac{1}{2}}^{1/2} i^{\mu} d^{1/2}_{1/2}(\mu)\left(\frac{\pi}{2}\right)\left|\frac{1}{2}\,\mu\right\rangle_z \\ &= \frac{1}{\sqrt{2}}\left(\left|\frac{1}{2}\,\frac{1}{2}\right\rangle_z + i\left|\frac{1}{2}-\frac{1}{2}\right\rangle_z\right) \\ &= \frac{1}{\sqrt{2}}(|10\rangle + i|01\rangle), \end{aligned} \tag{26}$$

where one finds again the $\pi/2$ phase shift between reflection and transmission. A twin-photon input $|11\rangle = |10\rangle_z$ gives

$$\begin{aligned} e^{i(\pi/2)J_x}|10\rangle_z &= \sum_{\mu=-1}^{1} i^{\mu} d^1_{0\mu}\left(\frac{\pi}{2}\right)|1\,\mu\rangle_z \\ &= \frac{i}{\sqrt{2}}(|11\rangle_z + |1-1\rangle_z) \\ &= \frac{i}{\sqrt{2}}(|20\rangle + |02\rangle). \end{aligned} \tag{27}$$

This is the well-known result that twin input photons always emerge together out of the same port of a lossless 50/50 beam splitter, the $|11\rangle = |10\rangle_z$ output state being suppressed by destructive quantum interferences [18].

2. Phase shift

A phase shift θ between the two ports a and b gives

$$\begin{pmatrix} a_{\rm out} \\ b_{\rm out} \end{pmatrix} = \begin{pmatrix} e^{i\theta/2} & 0 \\ 0 & e^{-i\theta/2} \end{pmatrix} \begin{pmatrix} a_{\rm in} \\ b_{\rm in} \end{pmatrix}, \tag{28}$$

and means a rotation of θ around z [Eq. (3) with, for example, $\alpha+\gamma=\theta, \beta=0$],

$$\boldsymbol{J}^{\rm out} = e^{i\theta J_z}\boldsymbol{J}^{\rm in}e^{-i\theta J_z}, \tag{29}$$

$$|\psi_{\rm out}\rangle = e^{-i\theta J_z}|\psi_{\rm in}\rangle, \tag{30}$$

which is consistent since a phase shift between fields a and b should affect the interference components J_x and J_y, but not the intensity difference J_z.

III. MACH-ZEHNDER INTERFEROMETER IN THE SCHWINGER REPRESENTATION

A. Description

The unitary operator for a Mach-Zehnder (Fig. 3) is the product of three operators corresponding to an input beam splitter, a phase shift, and an output beam splitter. This can be written, to an arbitrary phase choice left,

$$|\psi_{\rm out}\rangle = e^{-i(\pi/2)J_x}e^{i\theta J_z}e^{i(\pi/2)J_x}|\psi_{\rm in}\rangle = e^{-i\theta J_y}|\psi_{\rm in}\rangle, \tag{31}$$

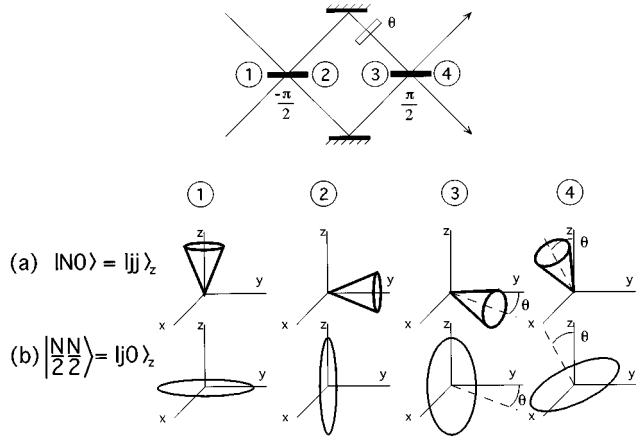

FIG. 3. The Mach-Zehnder interferometer and its action on the light states in the Schwinger representation. The different stages are numbered: 1 is the input, 2 is after the first beam splitter, 3 is after the phase shift, and 4 is after the second beam splitter. The intensity difference $N_a - N_b$ is given by the projection of $\boldsymbol{J}$ on the z axis, whereas the phase difference $\phi_a - \phi_b$ is given by the azimuthal angle of the projection of $\boldsymbol{J}$ in the (x,y) plane. The usual Heisenberg uncertainty between $J_{x,y}$ and J_z, graphically illustrated in (a) and (b), can thus be interpreted in terms of a number-phase uncertainty. (a) Evolution of the single-input Fock state $|jj\rangle$ in the Mach-Zehnder. The light state is a cone of side length $[j(j+1)]^{1/2}$, height j, and base radius $[j]^{1/2}$. (b) Evolution of the twin Fock state $|j0\rangle$ in the Mach-Zehnder. The light state is a disk of radius $[j(j+1)]^{1/2}$.

i.e., a rotation by the interferometer's phase shift θ around the y axis [$\alpha=\gamma=0, \beta=\theta/2$ in Eq. (3)]. For $\boldsymbol{J}$, the transformation is given by

$$\begin{pmatrix} J_x^{\text{out}} \\ J_y^{\text{out}} \\ J_z^{\text{out}} \end{pmatrix} = \begin{pmatrix} \cos\theta & 0 & -\sin\theta \\ 0 & 1 & 0 \\ \sin\theta & 0 & \cos\theta \end{pmatrix} \begin{pmatrix} J_x^{\text{in}} \\ J_y^{\text{in}} \\ J_z^{\text{in}} \end{pmatrix}. \tag{32}$$

It is worth noting that $\boldsymbol{J}$ undergoes the exact same rotations as the Bloch vector in a basic Ramsey fringes [19] experiment, and that there is a complete analogy between the two situations. The two complex probability amplitudes associated with each atomic state in a Ramsey fringes experiment are analogous to the two complex field amplitudes associated with each optical path a and b. The two $\pi/2$ laser pulses are having the exact same effect as the beam splitters, and, between them, the different phase evolutions of the two atomic states are the equivalent of the phase shift inside the Mach-Zehnder interferometer.

B. Fundamental limits of interferometric measurements

Figures 3(a) and 3(b) display the evolution of the light states in the interferometer for the single-input state $|jj\rangle_z$ (cone) and the twin-input state $|j0\rangle_z$ (disk). These geometrical representations simply illustrate the Heisenberg uncertainties (12) between the components of the angular momentum of the Schwinger representation.

We now interpret Figs. 3(a) and 3(b) using Eq. (13) (explicit derivations will be given in the next section). For any state, the intensity difference $N_a - N_b$ is given by the projection of $\boldsymbol{J}$ along the z axis, whereas the phase difference $\phi_a - \phi_b$ is the azimuthal angle of the projection of $\boldsymbol{J}$ in the (xy) plane. Figures 3(a) and 3(b) display two different types of Fock states: the single input [Eq. (17)] and the twin input [Eq. (18)]. In both cases, the phase difference $\phi_a - \phi_b$ is not defined at the input (region 1). But what is important is how well $\phi_a - \phi_b$ can be defined *after the first beam splitter*, where one probes the unknown phase shift θ [which is a real parameter: the Euler angle β of Eq. (3)]. From Heisenberg uncertainty (13), a minimum $\Delta(\phi_a - \phi_b)$ after the input beam splitter is equivalent to a maximum $\Delta(N_a - N_b)$ at the same point. Now, from the physics of the beam splitter discussed in Sec. II B 1 and displayed in Figs. 3(a) and 3(b), it is clear that a maximum intensity uncertainty *after* the beam splitter is obtained from a maximum phase uncertainty *before* it, because of the $\pi/2$ rotation of the state.

In the case of a single-port input (cone), the Pythagorean theorem and Fig. 3(a) tell us that the input phase fluctuations are $\Delta J_{x,y} = \sqrt{j}$. After the beam splitter, it is ΔJ_z that assumes this value, giving the SL

$$\Delta(\phi_a - \phi_b) \geqslant \frac{1}{\Delta(N_a - N_b)} = \frac{1}{2\sqrt{j}} = \frac{1}{\sqrt{2N}}. \tag{33}$$

In the case of a twin-photon input (disk), it is clear that the situation is the most favorable possible: the phase fluctuations at the input are maximized, which makes them very small inside the interferometer. In fact, the intensity uncertainty there is at its absolute maximum, in the sense that one cannot tell whether *all* the photons are in one arm or in the other. This is of course consistent with the usual quantum interferometry statement: the fringes are destroyed if one tries to find out which path the particle has taken. Here, all the particles are contributing, which should yield the highest possible sensitivity. Figure 3(b) shows indeed that

$$\Delta(\phi_a - \phi_b) \geqslant \frac{1}{\Delta(N_a - N_b)} = \frac{1}{2\sqrt{j(j+1)}} \sim \frac{1}{N}. \tag{34}$$

Finally, the second beam splitter restores minima fluctuations on the observable J_z^{out} (measured by subtracting the two output intensities), and detection of θ can be done at the HL *provided that* $\theta \sim 0$ (or a multiple of π). The Heisenberg-limited sensitivity is therefore not independent of θ [20]. It is indeed easy to see that, when $\theta = \pi/2$, the whole Mach-Zehnder is equivalent to a single beam splitter, which maximizes ΔJ_z^{out} and consequently the measurement error.

C. Phase measurements with twin photons

In this section, we give a rigorous derivation of the precision and signal-to-noise ratio of an interferometric measurement with quantum correlated photons.

1. What is to be measured?

From Fig. 3 or a simple calculation, the expectation value of the difference of the output intensities is given by

$$\langle J_z \rangle_z^{\text{out}} = {}_z\langle jj | (\sin\theta) J_x + (\cos\theta) J_z | jj \rangle_z = j\cos\theta, \tag{35}$$

for a single-port input, and by

$$\langle J_z\rangle_z^{\text{out}} = {}_z\langle j0|(\sin\theta)J_x+(\cos\theta)J_z|j0\rangle_z = 0, \quad \forall\,\theta, \quad (36)$$

for a twin-photon input. This means that, in the latter case, the average of the difference of the output intensities contains no information about the phase shift [21]. This is actually also true of the average output intensities:

$$\langle N_a\rangle_z^{\text{out}} = j+\langle J_z\rangle_z^{\text{out}} = j, \quad (37)$$

$$\langle N_b\rangle_z^{\text{out}} = j-\langle J_z\rangle_z^{\text{out}} = j. \quad (38)$$

This phase-nondependence of the average output intensities has been observed experimentally by Ou *et al.* [22]. The physical interpretation of this effect is that, at each output port, the dark fringe created by one input port is superimposed on the bright fringe created by the other input port, and, since the two fringes vary in opposite ways with θ, the total intensity at one output port keeps constant whatever θ is.

However, this concerns the second-order (field amplitude) correlation only. There obviously exists, in this case, a fourth-order (field intensity) correlation since the intensity difference is squeezed. This fourth-order correlation can be described by J_z^2, since

$$\langle :N_aN_b:\rangle_z = \frac{1}{2}[\langle J_z^2\rangle_z^{\text{out}} - \langle N_a^2\rangle_z - \langle N_b^2\rangle_z], \quad (39)$$

and we have just seen that the last two terms of the right side of Eq. (39) are independent of θ [Eqs. (37) and (38)]. Hence, all the phase information is contained in the variance $\langle J_z^2\rangle_z = (\Delta J_z)^2$, the square of the projection on the z axis of the uncertainty disk on Fig. 3(b). One has

$$\langle J_z^2\rangle_z^{\text{out}} = {}_z\langle j0|[(\sin\theta)J_x+(\cos\theta)J_z]^2|j0\rangle_z = \frac{\sin^2\theta}{2}j(j+1). \quad (40)$$

Therefore, a possible measurement scheme could simply be to measure this variance instead of $\langle J_z\rangle_z^{\text{out}}$ [23]. By squaring and integrating the output intensity difference signal, one would measure the expectation value of $S=4J_z^2$. A spectrum analyzer can perform these operations, with different levels of integration and the possibility to access the standard deviation $\Delta S = 4\Delta(J_z^2)$ as well.

We now derive the phase uncertainty and signal-to-noise ratio of such a measurement.

2. Phase sensitivity of a measurement of J_z^2

One can calculate the standard deviation of the measured phase shift θ, $\Delta\theta$, as a function of $\langle S\rangle$ and ΔS:

$$\Delta\theta = \frac{\Delta S}{\frac{d}{d\theta}\langle S\rangle} = \frac{\sqrt{\langle J_z^4\rangle_z^{\text{out}} - \langle J_z^2\rangle_z^{\text{out}\,2}}}{\frac{d}{d\theta}\langle J_z^2\rangle_z^{\text{out}}}. \quad (41)$$

A straightforward angular momentum calculation gives

$$\langle J_z^4\rangle_z^{\text{out}} = \frac{\sin^2\theta}{8}j(j+1)\{3\sin^2\theta[j(j+1)-2]+4\}. \quad (42)$$

and

$$\frac{d}{d\theta}\langle J_z^2\rangle_z^{\text{out}} = (\sin\theta)(\cos\theta)j(j+1). \quad (43)$$

Therefore,

$$(\Delta\theta)^2 = \frac{\tan^2\theta}{8} + \frac{1}{2j(j+1)\cos^2\theta}, \quad (44)$$

where one finds, as in Fig. 3(b), that $\Delta\theta$ is minimum when $\theta\sim 0$, and gives the HL:

$$\Delta\theta = \frac{1}{\sqrt{2j(j+1)}} \simeq \frac{\sqrt{2}}{N}. \quad (45)$$

3. Signal-to-noise ratio of a measurement of J_z^2

From Eqs. (42) and (40),

$$\frac{(\Delta S)^2}{\langle S\rangle^2} = \frac{1}{2} - \frac{3}{j(j+1)} + \frac{8}{\langle S\rangle} \simeq \frac{1}{2} + \frac{8}{\langle S\rangle}. \quad (46)$$

According to Eq. (40), $\langle S\rangle/\Delta S = 0$ if $\theta = 0$. If $\theta \gg 1/j$ (which is possible even though one needs $\theta\sim 0$ rad example: $\theta = 1\,\mu$rad, $j=10^8$), then $1/\langle S\rangle$ becomes negligible and the maximum signal-to-noise is

$$\frac{\langle S\rangle}{\Delta S} = \sqrt{2}, \quad (47)$$

which indicates that determining θ by measuring the noise on the output difference, $\langle J_z^2\rangle$, may not be the best way to proceed, considering also that we have assumed here ideal experimental conditions.

Ou *et al.* [22] have obtained an excellent signal-to-noise by using coincidence detection of the twin photons emitted by PDC [i.e., by measuring the left side of Eq. (39), $\langle :N_aN_b:\rangle$, rather than $\langle J_z^2\rangle$]. The signal-to-noise is better because only coinciding photons at the detectors are taken into account. The signal level is therefore maximum when $\theta = n\pi$ and zero when $\theta = (2p+1)\pi/2$, according to Fig. 3. Such a photon-by-photon detection requires the counting resolution time to be much smaller than the typical time between consecutive incoming photons. In Ref. [22], the parametric down-converter bare crystal gave close to a 100% correlation, but very low intensities for the signal and idler beams (3600 counts/s). Therefore, the 13-ns resolution time used insured a good signal-to-noise. However, for ultimate-sensitivity phase measurements such as gravitational-wave detection, one clearly needs large numbers of photons, as given by an OPO, which has a much higher photon emission rate than PDC. In this case, the resolution time needed for a count detection is impossible to reach (much less than 1 ns). Besides, since the resonator buildup means a much narrower emission linewidth, an OPO photon pair can be, once created in the crystal, temporally separated because the two photons can exit the OPO cavity at different times. It is therefore necessary, in order to collect the maximum of correlated photons on the detectors, that a measurement last typically as long as the storage time of the OPO cavity. Because of both

this loss of time resolution and this need to integrate, the detection method has to be a frequency-domain one.[3]

To summarize, a direct measurement of the output difference intensity, J_z^{out}, provides no information about θ [Eq. (36)]. A direct measurement of the variance of J_z^{out}, $(J_z^{\text{out}})^2$, is phase sensitive [Eq. (40)], but presents a standard deviation of the order of the measurement result [Eq. (47)], that will require averaging a very large number of independent measurements[4] to obtain a decent signal-to-noise ratio.

IV. HEISENBERG-LIMITED PHASE MEASUREMENTS IN NONIDEAL EXPERIMENTAL CONDITIONS

The problem of the extremely low signal-to-noise of Eq. (47) can be overcome by using a data processing method based on a Bayesian analysis of the output of the interferometer. We first give a brief review of this method [9], before we model realistic experimental conditions.

A. Measurement method

It is a nonlinear measurement method and is therefore not based on averaging. Its principle is to pick a few independent realizations of J_z^{out}, and reconstruct the probability distribution for each of them. Since the measurements are independent, the joint probability of all of them is the product of all the previously reconstructed distributions, which has a single, narrow peak.

Equation (36) can be rewritten in terms of probabilities,

$$\langle J_z\rangle_z^{\text{out}} = \sum_{\mu,\mu'} \langle\psi_{\text{out}}|j\mu\rangle_{zz}\langle j\mu|J_z|j\mu'\rangle_{zz}\langle j\mu'|\psi_{\text{out}}\rangle$$

$$= \sum_{\mu} |{}_z\langle j\mu|\psi_{\text{out}}\rangle|^2\mu = 0. \quad (48)$$

Contrary to the above average, a single measurement of J_z gives neither a null result nor a result independent of θ, but the result μ, with the probability

$$P(\mu|\theta,j) = |{}_z\langle\ j\mu|\psi_{\text{out}}\rangle|^2 = |{}_z\langle j\mu|e^{i\theta J_y}|j0\rangle_z|^2. \quad (49)$$

In the case of a perfectly correlated input [Eq. (18)], the probability depends on an associated Legendre polynomial

$$P(\mu|\theta,j) = [d^j_{\mu 0}(\theta)]^2 = \frac{(j-\mu)!}{(j+\mu)!}[P_j^{\mu}(\cos\theta)]^2. \quad (50)$$

If one performs p *statistically independent* measurements of μ, at j and θ fixed, then the global probability distribution [9] is given by the Bayes theorem [24]

$$P(\theta|\mu_1 \text{ and } \cdots \text{ and } \mu_p, j) \propto \prod_{i=1}^{p} P(\mu_i|\theta,j)$$

$$= \prod_{i=1}^{p} [d^j_{\mu 0}(\theta)]^2. \quad (51)$$

One should note that this method only gives access to the absolute value of the phase shift, since changing the sign of θ does not change Eqs. (49)–(51). This is because the measurement result depends on quantum probabilities and not amplitudes.

It is also important to define *independent* measurements from the experimental point of view: the key parameter here is the correlation bandwidth of the photon pairs, which is given by the emission linewidth (inverse of the storage time τ_c) of the OPO that produces them. As we mentioned earlier, a typical measurement time τ will have to be $\geqslant \tau_c$. Increasing τ will then allow one to collect more photons, thereby increasing the resolution of the measurement. τ will ultimately be limited by the time constant characteristic of photon loss processes in the OPO, τ_l.[5] If the interval between two measurements is $\gg \tau_l$, then the OPO losses will decorrelate the photons of the two measurements enough to ensure their independence.

B. Simulation method and results

1. Influence of photon statistics

Using the density matrix, one can write the general form

$$\rho = \sum_{N,N'} c_{NN'} \left|\frac{N}{2}\,\frac{N}{2}\right\rangle\left\langle\frac{N'}{2}\,\frac{N'}{2}\right|$$

$$= \sum_{j,j'} c_{jj'}|j0\rangle_{zz}\langle j'0|. \quad (52)$$

We call the input state $|j0\rangle_z$ of Eq. (18) a Fock twin-photon state. Its statistics are trivial: $c_{jj'} = \delta_{j',j}\delta_{j,N/2}$. We define the coherent twin-photon state, or coherent pair, by $\rho = |\alpha\alpha\rangle\langle\alpha\alpha|$ with

$$c_{jj'} = e^{-|\alpha|^2}\frac{\alpha^j\alpha^{*j'}}{\sqrt{j!j'!}}, \quad (53)$$

$|\alpha|^2 = \overline{N}/2$ being the average number of photons per port. Finally, we define thermal pairs by

$$c_{jj'} = \frac{m^j}{(1+m)^{1+j}}\delta_{jj'}, \quad (54)$$

$m = \overline{N}/2$ being the average number of photons per port.

[3] These two situations, OPO and PDC, are in fact Fourier transforms of each other: the emission linewidth, which is also the quantum correlation linewidth, is broad for PDC (phase-matching linewidth) and narrow for OPO (buildup cavity linewidth); and detection is a time cross-correlation of the two photodetectors for PDC (coincidence counting) and a cross-spectrum for OPO.

[4] If the ith measurement is described by the random variable X_i, whose average is $\overline{X_i} = \overline{X}, \forall i$, and standard deviation $\sigma_i = \sigma_X, \forall i$, then an *n-averaged measurement*, described by the random variable $Y = \Sigma_{i=1}^n X_i/n$, has the same average, $\overline{Y} = \overline{X}$, and the smaller standard deviation $\sigma_Y = \sigma_X/\sqrt{n}$.

[5] $\tau_l \gg \tau_c$ being required in order to obtain highly quantum-correlated OPO outputs [25].

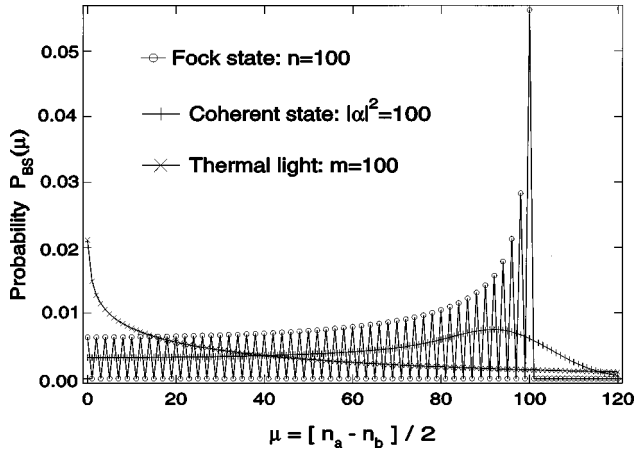

FIG. 4. Output distribution of the beam splitter. Average input: 100 photons/port.

It is interesting to visualize what the Fock, Poisson, and Planck distributions become after the input beam splitter of the interferometer. From $\langle J_z\rangle_z^{\text{out}}=\text{Tr}[\rho J_z^{\text{out}}]$ and $\theta=\pi/2$, the beam splitter probability distributions are

$$P_{\text{BS}}(\mu)=\sum_{j=0}^{\infty} c_{jj}P\left(\mu\left|\frac{\pi}{2},j\right.\right). \tag{55}$$

Results of a calculation for $\bar{N}/2=100$ input photons in each port are plotted in Fig. 4 for $\mu\geqslant 0$ only, $P(\mu|\theta,j)$ being even with respect to μ. The output distribution for a Fock twin-photon state [26] with $j=100$ input photons should be compared to Eq. (27) for a single input photon: there is still a peak at $\mu=j$, which signals that the most probable outputs are $|2j\ \ 0\rangle$ and $|0\ \ 2j\rangle$, like the output in Eq. (27). Other outputs are possible, only with even numbers: $|2j-2\ \ 2\rangle$, $|2j-4\ \ 4\rangle$, etc. A coherent input state gives a result very close to the Fock state, except that odd numbers of photons are also possible. Finally, the thermal distribution gives a significantly different shape, but still the same *spread*, of order j and not $\sqrt{j}$ (as in the single input case), which is the important point here. If one remembers that a beam splitter is actually equivalent to the Mach-Zehnder with a phase shift $\theta=\pi/2$, one can connect Fig. 4 to Fig. 3: because of the spread of the photon distribution as displayed in Fig. 4, the fluctuations of J_z are maximized, and therefore the informational content (on θ) of the measurement is lost. These fluctuations do not depend on the type of statistics of the light: the spread of the distributions in Fig. 4 is always of the order j and has nothing to do with the input shot noise.

Hence, a reasonable assumption is that the *common-mode* photon statistics of the input beams should have no influence on the ultimate sensitivity of phase-shift measurements. We have simulated this case for $p=10$ measurements, each containing an average of 100 photons, that is, $j=100$ for a Fock state, $|\alpha|^2=100$ for a coherent state, and $m=100$ for thermal light. The simulation procedure went as follows: we scanned the phase shift of the interferometer ($\theta_s=1$ mrad to 1 rad), and for each value of θ_s we simulated 10 statistically independent measurement results for the difference of the output intensities J_z. For each measurement $i=1$ to 10, the input photon number was randomly picked from a Poisson or Planck distribution, or taken equal to 100 for a Fock state. This gave a value j_i. The corresponding input state $|j_i j_i\rangle$ was then fed into the interferometer, i.e., a measurement result for J_z, $\mu_i(\theta_s,j_i)$, was randomly picked using the distribution of Eq. (50) at the current values of θ_s and j_i. Putting ourselves now in the place of the measurer, who *does not know* θ_s, but has just measured the couple (j_i,μ_i), we can reconstruct a probability distribution for θ, which is the function $P(\mu_i(\theta_s,j_i)|\theta,j_i)$ from Eq. (50), but with θ as a variable. Repeating the operation for every measurement yields ten such distributions, which are then multiplied, according to Eq. (51), to obtain a global distribution for all ten measurements. This final, sharp-peaked, distribution is used to calculate the average and standard deviation of θ:

$$\bar{\theta}=\int \frac{d\theta}{\theta P(\mu_1(\theta_s,j_1)\ \text{ and }\ \cdots\ \text{ and }\ \mu_{10}(\theta_s,j_{10})|\theta,\bar{j})}=\theta_s, \tag{56}$$

$$\Delta\theta=\left\{\int \frac{d\theta}{(\theta-\bar{\theta})^2 P(\mu_1(\theta_s,j_1)\ \text{ and }\ \cdots\ \text{ and }\ \mu_{10}(\theta_s,j_{10})|\theta,\bar{j})}\right\}^{1/2}. \tag{57}$$

Figure 5 displays $\Delta\theta$ versus θ_s for the aforementioned conditions and the three different types of light. All plots have been averaged to get rid of spurious numerical fluctuations (this was also achieved by adding several complete simulations). It is clear that photon statistics do not play any role here, and that all that happens is related to the physics of the interferometer (more precisely of the beam splitter). One can also see the confirmation of the analysis in Secs. III B (Fig. 3) and III C [Eq. (44)]: the spread of the photon distribution narrows down to the HL when $\theta=0$, and blows up well past the SL when $\theta\rightarrow\pi/2$. The numerical simulations place the HL at $\Delta\theta=1.4\times10^{-3}$ rad, close to the result of [Eq. (45)]: $\Delta\theta=\sqrt{2}/pN=0.7\times10^{-3}$ rad. One can remark that this result is p times better than the HL of a single measurement, instead of the usual improvement by $\sqrt{p}$ that one obtains by averaging. This is because the method really makes use of the photons in all p measurements to — nonlinearly — determine $\Delta\theta$, rather than — linearly — averaging p independent determinations of $\Delta\theta$.

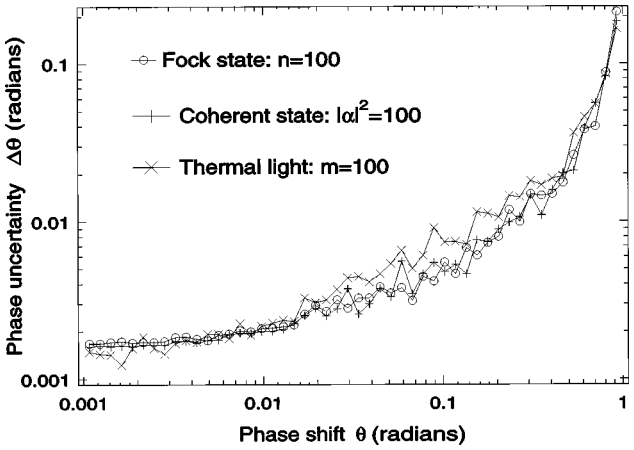

FIG. 5. Standard deviation of phase-shift measurements for different photon statistics.

2. Partial correlation of the two-port input of the interferometer: Influence of the intensity-difference squeezing level of the OPO

For this analysis, we have used an unbalanced coherent input $|n_a n_b\rangle = |j\nu\rangle_z$. In this case, more general than Eq. (50), the Mach-Zehnder rotation matrix element involves a Jacobi polynomial instead of a Legendre polynomial,

$$P(\mu|\theta,j,\nu) = |{}_z\langle j\mu|e^{i\theta J_y}|j\nu\rangle_z|^2 = [d^j_{\mu\nu}(\theta)]^2 = \frac{(j+\mu)!(j-\mu)!}{(j+\nu)!(j-\nu)!}\left[\cos\frac{\theta}{2}\right]^{2(\mu+\nu)}\left[\sin\frac{\theta}{2}\right]^{2(\mu-\nu)} \times [P^{(\mu-\nu,\mu+\nu)}_{j-\mu}(\cos\theta)]^2, \quad (58)$$

where $\mu = (n_a^{\text{out}} - n_b^{\text{out}})/2$, as before, and $\nu = (n_a^{\text{in}} - n_b^{\text{in}})/2$. To simulate this case, we have started from the exact same procedure as in the preceding section. Since the issue here is clearly related to the use of an OPO above threshold, we have assumed Poissonian statistics ($|\alpha|^2 = 100$) and added a binomial test between the random pick of the input photon number j_i (now n_{ia}, for port a) and the interferometer step. The binomial probability is the degree of photon correlation. If the binomial test result is ''correlated,'' then we assign $n_{ib} = n_{ia}$, otherwise n_{ib} is determined by a new random pick from the same Poissonian distribution. The created $|n_{ia} n_{ib}\rangle = |j_i \nu_i\rangle_z$ is then used in Eq. (58) to create a measurement result μ_i. The rest of the procedure is identical to Fig. 5. Results are plotted on Fig. 6. It is clear from Fig. 6 that the destruction of the photon correlation leads to a return to the SL, which the simulation places at $1/\sqrt{2pN}$. A 0% correlation is equivalent to two independent lasers input into each port of the Mach-Zehnder. With 100 photons, 70% at least of intensity-squeezing is required to start to obtain sub-SL sensitivity. However, it is important to note here that 100 photons is an unrealistically small number, required to be able to carry out the Jacobi polynomial calculation. Even a small OPO output power, for example 1 mW at 1064 nm, already gives 5×10^9 photons per measurement, assuming an OPO linewidth of 1 MHz. Numerical simulations become impossible to carry out at these numbers, and asymptotic expansions are not very useful because they place restrictions on the possible values for μ and ν. One question left open is therefore to ascertain how $\Delta\theta$ scales, between $N^{-1/2}$ and N^{-1}, when N increases. If the scaling law is faster than $N^{-1/2}$, then the same degree of correlation will produce much better results with 10^9 photons than in this 100-photon simulation.

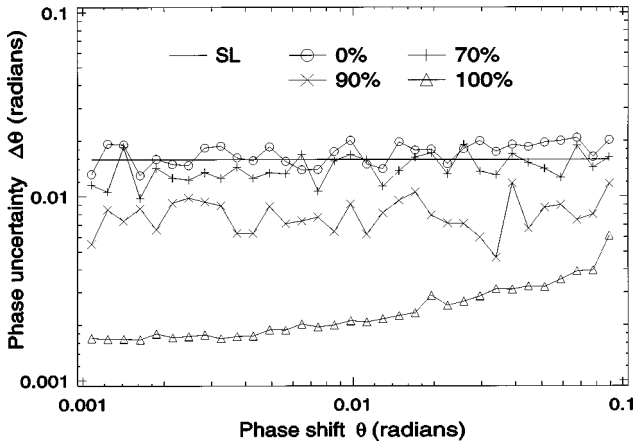

FIG. 6. Standard deviation of phase-shift measurements for differently correlated coherent input states.

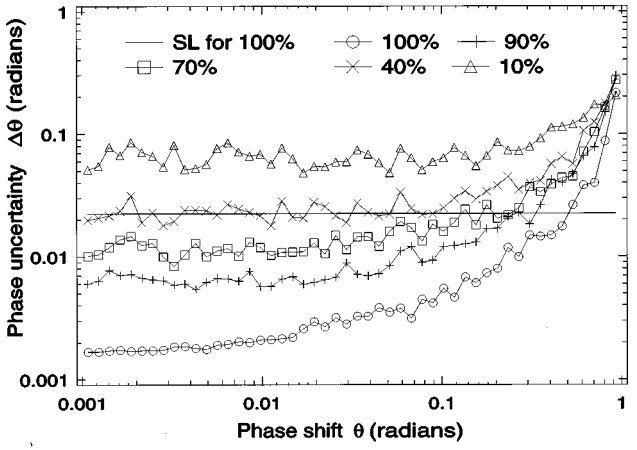

FIG. 7. Standard deviation of phase-shift measurements for different quantum efficiencies of the photodetectors at the output of the Mach-Zehnder.

3. Partial correlation of the two-port output of the interferometer: Influence of the quantum efficiency of the photodetectors

This case is treated with the procedure used for the study of photon statistics [perfectly correlated Fock input, distribution of Eq. (50)]. We added a binomial test before the reconstruction of the phase distribution from the measured (j_i, μ_i): the binomial probability is this time essentially the quantum efficiency of the photodetectors, η. The test is independently applied to the output photon numbers n_{ia} and n_{ib} at each port, given from (j_i, μ_i) by Eq. (15). One obtains then two new n'_{ia} and n'_{ib}, i.e., a modified (j'_i, μ'_i) that is finally used to reconstruct the probability for the measurement. The standard deviation is plotted in Fig. 7. It is worth noting here that, contrary to what it seems, $\Delta\theta$ never exceeds the SL (for $\theta = 0$) because a nonunity quantum detecting efficiency not only leads to photon pair decorrelation, but also to a reduction of the total number of photons $N' = 2j'$.

This increases the SL and the HL from their initial values, plotted in Fig. 7. For example, $\eta=10$ (photomultiplier) leaves us with $pN'=200$ detected photons, from the input $pN=2000$ (10 measurements $\times 100$ photons/port $\times 2$ ports). The SL is hence 5.0×10^{-2} instead of 1.6×10^{-2}.

V. CONCLUSION

We have extensively studied the influences of imperfect experimental parameters on a Heisenberg-limited interferometric measurement scheme. We point out that the major difficulty of this scheme is the detection, as our estimation of the signal-to-noise of a direct detection of J_z^2 shows, and that this difficulty is solved by the use of a Bayesian analysis of the data. By use of computer simulations mimicking what the experimental data processing should be, we have studied the influence of photon statistics, as well as of random deletion of photon pairs, before (decorrelation) and after (quantum efficiency) the interferometer. As for the SL, the HL does not depend on the input photon statistics: both are fixed by the physics of the beam splitter. The critical experimental parameters are θ, which has to be close to a multiple of π, and of course the rate of squeezing, i.e., of photon correlation. Intensity-difference squeezing is promising because the rate of squeezing is one of the highest that has been obtained up to now [25,27]. Although the extensive character of this study restrained it to very small numbers of photons, the results show that reasonable improvements beyond the SL are to be expected using quantum correlated photons, even in nonideal experimental conditions. We are currently pursuing the experimental investigation of this measurement, at different light powers, in order to settle the question of the scaling of $\Delta\theta$ with N at constant correlation. Also, as we noted in the Introduction, these results can easily be generalized to matter-wave boson interferometers.

ACKNOWLEDGMENTS

We are deeply grateful to Marc D. Levenson for his valuable insight and input during many fruitful discussions. This work was supported by the Office of Naval Research and NIST.

[1] M. Born and E. Wolf, *Principles of Optics*, 6th ed. (Pergamon Press, Oxford, 1989).
[2] C. M. Caves, Phys. Rev. Lett. **45**, 75 (1980).
[3] C. M. Caves, Phys. Rev. D **23**, 1693 (1981).
[4] R. S. Bondurant and J. H. Shapiro, Phys. Rev. D **30**, 2548 (1984).
[5] M. Xiao, L.-A. Wu, and H. J. Kimble, Phys. Rev. Lett. **59**, 278 (1987).
[6] P. Grangier, R. E. Slusher, B. Yurke, and A. LaPorta, Phys. Rev. Lett. **59**, 2153 (1987).
[7] B. Yurke, S. L. McCall, and J. R. Klauder, Phys. Rev. A **33**, 4033 (1986).
[8] H. P. Yuen, Phys. Rev. Lett. **56**, 2176 (1986).
[9] M. J. Holland and K. Burnett, Phys. Rev. Lett. **71**, 1355 (1993).
[10] B. C. Sanders and G. J. Milburn, Phys. Rev. Lett. **75**, 2944 (1995).
[11] C. Brif and A. Mann, Phys. Rev. A **54**, 4505 (1996).
[12] J. J. Bollinger, W. M. Itano, D. J. Wineland, and D. J. Heinzen, Phys. Rev. A **54**, R4649 (1996).
[13] P. Bouyer and M. Kasevich, Phys. Rev. A **56**, R1083 (1997).
[14] D. F. Walls and G. J. Milburn, *Quantum Optics* (Springer-Verlag, Berlin, 1994); R. Loudon, *The Quantum Theory of Light*, (Oxford University Press, Oxford, 1973); special issue on quantum phase, Phys. Scri. **T48** (1993), edited by W. P. Schleich and S. M. Barnett.
[15] L. C. Biedenharn and J. D. Louck, *Angular Momentum in Quantum Physics: Theory and Applications* (Addison-Wesley, Reading, MA 1981).
[16] J.-M. Lévy-Leblond and F. Balibar, *Quantics. Rudiments of Quantum Physics* (North-Holland, Amsterdam, 1990).
[17] M. Hillery, M. Zou, and V. Bužek, Quantum Semiclassic. Opt. **8**, 1041 (1996).
[18] C. K. Hong, Z. Y. Ou, and L. Mandel, Phys. Rev. Lett. **59**, 2044 (1987).
[19] M. D. Levenson, *Introduction to Nonlinear Laser Spectroscopy* (Academic Press, New York, 1982).
[20] This is not a general result for Heisenberg-limited phase measurements: Ref. [10] presents a general optimal measurement scheme where the precision is HL for all values of θ.
[21] This remark has also been made in Ref. [12], where the Heisenberg limit for frequency resolution in the spectroscopy of N trapped ions is investigated. The state to be used inside the interferometer (i.e., after the first beam splitter) is $|\psi_{\text{in}}\rangle=(1/\sqrt{2})[|jj\rangle+|j-j\rangle]$, with $j=N/2$ and where $\boldsymbol{J}$ is the coupling of N Bloch vectors. The equivalent state in our work is more complicated and displayed in Fig. 4.
[22] Z. Y. Ou, X. Y. Zou, L. J. Wang, and L. Mandel, Phys. Rev. A **42**, 2957 (1990).
[23] This detection strategy has been independently proposed in Ref. [13].
[24] C. W. Gardiner, *Quantum Noise* (Springer-Verlag, Berlin, 1991), p. 27.
[25] J. Mertz, T. Debuisschert, A. Heidmann, C. Fabre, and E. Giacobino, Opt. Lett. **16**, 1234 (1991).
[26] The Fock result only was also calculated in R. A. Campos, B. E. A. Saleh, and M. C. Teich, Phys. Rev. A **40**, 1371 (1989).
[27] D. T. Smithey, M. Beck, M. Belsey, and M. G. Raymer, Phys. Rev. Lett. **69**, 2650 (1992).